社団法人 情報処理学会 研究報告
IPSJ SIG Technical Report

2007－CVIM－157 (17)
2007／1／12

高次拘束によるオプティカルフローを利用した動きの分類

亀田 裕介† 井宮 淳††

† 千葉大学 自然科学研究科
†† 千葉大学総合メディア基盤センター
〒 263-8522 千葉市稲毛区弥生町 1-33

あらまし 本論文では, 高次微分拘束を利用した変分法によるオプティカルフロー計算を提案し、拘束の次数によって画面上点の動きを分類できることを示す. オプティカルフローはベクトル場であるため, 勾配法によるオプティカルフロー計算に, ベクトルスプライン拘束を採用することが行われる. また, 変形体の境界壁の動きの抽出には, 変形体の力学的性質から薄板スプライン拘束を利用することも行われる. 1 次ベクトルスプライン拘束は, Horn-Schunck 式に等価になる場合が知られている. また, 2 次ベクトルスプライン拘束が薄板スプラインと等価になる場合が知られている. そこで本論文では, 微分拘束の次数の違いと、支配される物理現象の違いとを利用して違いを利用して, 画面中の点の動きを分類する.

Motion Segmentation using the Higher Order Constraints for Optical-Flow Computation

Yusuke KAMEDA† and Atsushi IMIYA††

†School of Science and Technology, Chiba University
††Institute of Media and Information Technology, Chiba University
Yayoi-cho 1-33, Inage-ku, Chiba, 263-8522, Japan

Abstract In variational methods, a problem in computer vision and image analysis is expressed the summation of the data-term and the prior-term. The data-term is usually constructed from observed data. The prior-term defined by knowledges and assumptions on the problem acts as regulariser to the data-term of the problem. A typical class of prior-terms defines smoothness of the solution. In this paper, we deal with energy functional with the higher order derivatives for vector valued functions and show that it is possible to classify the motions in an image using variational optical-flow computation. We classify the motions of points in an image using the priors with various order differential- constraints. Using the first and second order derivatives, we show that variational method with the first order constraints accurately extracts optical-flow vectors in texture areas and that variational method with the second order derivatives derives the motion of segment-boundaries. Therefore, the results shows that it is possible to classify the texture regions and segment-boundaries in an image using the first and second derivatives as the constraints of optical-flow computation.

1 Introduction

Motion segmentation is a common problem in video-image processing and robot vision. In both cases, detection of moving objects and separation of them from stational background is a central problem, since this process derives a fundamental feature for motion understanding and separation. In motion tracking, separation and tracking of multiple motion is an essential problem. The other new area in motion analysis is classification of the motions and separation of motions based on classification.

In this paper, we deal with motion classification problem and show that it is possible to classify the motions in an image using variational optical-flow computation. We classify the motions of points in an image using the priors with various order differential- constraints.

The classical constraints for optical-flow computation is the quad Eric form of the first order derivatives [4, 5]. Recently, the second order vector-spline constraint is introduced to cloud-motion analysis for satellite images of typhoons. We have introduces a general theory of constraints with the higher order derivatives for optical flow computation. In this paper, we the difference of the optical-flow vectors depending on the orders the constraints in variational method for the optical-flow computation. Using the

first and second order derivatives, we show that variational method with the first order constraints accurately extracts optical-flow vectors in texture areas and that variational method with the second order derivatives derives the motion of segment-boundaries. Therefore, the results shows that it is possible to classify the texture regions and segment-boundaries in an image using the first and second derivatives as the constraints of optical-flow computation.

Section 2 is a mathematical preliminary. In section 3, we summarise a general theory of the higher order Horn-Schunck type constraints for optical flow. In section 4, we show some numerical results. Section 4 is devoted to discussion on mathematical properties of the algorithm.

2 Matrisation of Tensor

For the higher order derivatives, we describe a recursive construction rule. We set

$$\boldsymbol{H}_1 = \nabla f, \ \boldsymbol{H}_2 = \nabla\nabla^\top f. \tag{1}$$

Same as the Whitney array, we have the relation

$$\boldsymbol{H}_{k+1} = \begin{pmatrix} \partial_{x_1}\boldsymbol{H}_k \\ \partial_{x_2}\boldsymbol{H}_k \\ \vdots \\ \partial_{x_n}\boldsymbol{H}_k \end{pmatrix} = \nabla\boldsymbol{H}_k \tag{2}$$

for $k \geq 2$. We call $\boldsymbol{H}_k$ the k-th order Hessian. This relation implies the next proposition.

proposition 1. *The Hessian of the order k is constructed by the recursive form*

$$\boldsymbol{H}_{2k+1} = \nabla\boldsymbol{H}_{2k} \tag{3}$$
$$\boldsymbol{H}_{2k+2} = \nabla\boldsymbol{H}_{2k}\nabla^\top \tag{4}$$

for $k \geq 2$.

From this proposition, we have the next assertion.

assertion 1. *The size of* H_k *is* $n^p \times n^p$ *and* n^{p+1} *timesn*^{p} *for* $k = 2p$ *and* $k = 2p+1$, *respectively.*

We show examples. the third and fourth order Hessians of the scaler function on a plane are

$$\boldsymbol{H}_3 = \begin{pmatrix} f_{xxx} & f_{xxy} \\ f_{xyx} & f_{xyy} \\ f_{yxx} & f_{yxy} \\ f_{yyx} & f_{yyy} \end{pmatrix}, \tag{5}$$

$$\boldsymbol{H}_4 = \begin{pmatrix} f_{xxxx} & f_{xxyx} & f_{xxxy} & f_{xxyy} \\ f_{xyxx} & f_{xyyx} & f_{xyxy} & f_{xyyy} \\ f_{yxxx} & f_{yxyx} & f_{yxxy} & f_{yxyy} \\ f_{yyxx} & f_{yyyx} & f_{yyxy} & f_{yyyy} \end{pmatrix} \tag{6}$$

Geometrical Property of the Higher Order Hessian Matrix

Setting a coordinate transform to be

$$\boldsymbol{y} = \Phi(\boldsymbol{x}), \ y_i = \psi_i(x_1, x_2, \cdots, x_n) \tag{7}$$

the Hessian matrices $\hat{\boldsymbol{H}}$ and $\boldsymbol{H}$ with respect to the arguments *bmy* and $\boldsymbol{x}$, respectively, are combined by the relation

$$\hat{\boldsymbol{H}} = \boldsymbol{J}^\top\boldsymbol{H}\boldsymbol{J}, \tag{8}$$

where $\boldsymbol{J}$ is the Jacobian matrix of the transform Φ. Specially, if the transformation is linear,

$$\boldsymbol{y} = \boldsymbol{A}\boldsymbol{x}, \tag{9}$$

we have the relations

$$\hat{\boldsymbol{H}}_3 = diag(\boldsymbol{A}^\top, \boldsymbol{A}^\top)\boldsymbol{H}_3\boldsymbol{A} \tag{10}$$
$$\hat{\boldsymbol{H}}_4 = diag(\boldsymbol{A}^\top, \boldsymbol{A}^\top)\boldsymbol{H}_4 diag(\boldsymbol{A}, \boldsymbol{A}) \tag{11}$$

Furthermore, If $\boldsymbol{A}^\top\boldsymbol{A} = \boldsymbol{I}$, the Hessian matrices $\hat{\boldsymbol{H}}$ and $\boldsymbol{H}$ satisfy the relation

$$tr\boldsymbol{H}\boldsymbol{H}^\top = tr\hat{\boldsymbol{H}}\hat{\boldsymbol{H}}^\top. \tag{12}$$

Next, we investigate generalisations of these relations to the higher order Hessian tensor.

For the k-th order Hessian matrix, we have the next proposition.

proposition 2. *If* $\boldsymbol{y} = \boldsymbol{A}\boldsymbol{x}$, *that is* $y_i = \sum_{j=1}^n a_{ij}x_j$, *we have the relation*

$$\hat{\boldsymbol{H}}_k = \boldsymbol{L}_k\boldsymbol{H}_k\boldsymbol{R}_k \tag{13}$$

where

$$\boldsymbol{L}_{2k-1} = \boldsymbol{L}_{2k} = d^k(\boldsymbol{A}^\top), \ \boldsymbol{R}_{2k} = \boldsymbol{R}_{2k+1} = d^k(\boldsymbol{A}), \ k \geq 1 \tag{14}$$

for

$$d^{k+1}(\boldsymbol{X}) = diag(\boldsymbol{X}d^k(\boldsymbol{X}), \boldsymbol{X}^{k+1}), \ d^1(\boldsymbol{X}) = \boldsymbol{X}, \ k \geq 1. \tag{15}$$

(Roof) From eqs. (3) and (4), we have

$$\hat{\boldsymbol{H}}_{2k+1} = \hat{\nabla}\boldsymbol{H}_{2k} = \boldsymbol{A}^\top\nabla\boldsymbol{H}_{2k} \tag{16}$$
$$\hat{\boldsymbol{H}}_{2k+2} = \hat{\nabla}\boldsymbol{H}_{2k}\hat{\nabla}^\top = \boldsymbol{A}^\top\nabla\boldsymbol{H}_{2k}\nabla^\top\boldsymbol{A} \tag{17}$$

for $k \geq 2$, where $hat\nabla$ is the gradient with respect to $\boldsymbol{y} = (y_1, y_2, \cdots, y_n)^\top$, Since for $k = 1, 2$ $\hat{\nabla} = \boldsymbol{A}^\top\nabla$ and $\boldsymbol{A}^\top\boldsymbol{H}\boldsymbol{A}$, respectively, we have eq. (13). (Q.E.D)

From this proposition, we have the next proposition as well.

proposition 3. *The Frobenius norm of the k-th order Hessian matrix of a scaler function is rotation invariant, that is,*

$$tr\hat{\boldsymbol{H}}_k\hat{\boldsymbol{H}}_k{}^\top = tr\boldsymbol{H}_k\boldsymbol{H}_k^\top \tag{18}$$

Therefore, we have the next proposition for the k-th order Hessian matrix of the vector function.

proposition 4. *The Frobenius norm of the k-th order Hessian matrix of the vector function is rotation invariant, that is,*

$$tr\hat{\boldsymbol{H}}_k\hat{\boldsymbol{H}}_k{}^{\top} = tr\boldsymbol{H}_k\boldsymbol{H}_k^{\top} \tag{19}$$

For a unitary matrix $\boldsymbol{W}$, setting

$$\boldsymbol{v}(\boldsymbol{x}) = \boldsymbol{W}\boldsymbol{u}(\boldsymbol{x}), \tag{20}$$

we have the relation

$$D^k\boldsymbol{v} = diag(\boldsymbol{W}, \boldsymbol{W}, \cdots, \boldsymbol{W})D^k\boldsymbol{u}. \tag{21}$$

Since

$$D^k f^{\top} D^k f = tr\boldsymbol{H}_k\boldsymbol{H}_k^{\top} \tag{22}$$

and

$$diag(\boldsymbol{W}, \boldsymbol{W}, \cdots, \boldsymbol{W})^{\top} = diag(\boldsymbol{W}, \boldsymbol{W}, \cdots, \boldsymbol{W}) = \boldsymbol{I}, \tag{23}$$

we have the next proposition.

proposition 5. *For the k-th order Hessian of vector functions, the relation*

$$tr\boldsymbol{H}_k(\boldsymbol{v})\boldsymbol{H}_k(\boldsymbol{v}) = tr\boldsymbol{H}_k(\boldsymbol{u})\boldsymbol{H}_k(\boldsymbol{u}) \tag{24}$$

is satisfied, where $\boldsymbol{H}_k(\boldsymbol{u})$ and $\boldsymbol{H}_k(\boldsymbol{v})$ are the k-th order Hessian of $\boldsymbol{u}$ and $\boldsymbol{v}$, respectively.

3 Optical Flow Computation

Optical flow of images defines the vector field. Therefore, the vector-spline regularisation is used for the stable optical-flow computation [14].

The optical-flow computation with the second order constraint is

$$\begin{aligned} J_{\alpha\beta}(\boldsymbol{u}) &= \int_{\mathbf{R}^3} \{|\nabla f^{\top}\boldsymbol{u} + f_t|^2 \\ &\quad + \alpha tr\nabla\boldsymbol{u}\nabla\boldsymbol{u}^{\top} + \beta tr\boldsymbol{H}\boldsymbol{H}^{\top}\}\, d\boldsymbol{x}. \end{aligned} \tag{25}$$

The Euler-Lagrange equation of the variational problem is

$$\frac{\beta}{\alpha}\Delta^2\boldsymbol{u} - \Delta\boldsymbol{u} + \frac{1}{\alpha}(\nabla f^{\top}\boldsymbol{u} + f_t)\nabla f = 0, \tag{26}$$

and its embedding into evolution equation is

$$\frac{\partial}{\partial\tau}\boldsymbol{u} = -\frac{\beta}{\alpha}\Delta^2\boldsymbol{u} + \Delta\boldsymbol{u} - \frac{1}{\alpha}(\nabla f^{\top}\boldsymbol{u} + f_t)\nabla f. \tag{27}$$

Furthermore, for $tr\boldsymbol{H}_{\boldsymbol{u}}\boldsymbol{H}_{\boldsymbol{u}}^{\top}$, we have the relation

$$tr\boldsymbol{H}\boldsymbol{H}^{\top} = |\nabla div\boldsymbol{u}|^2 + |\nabla rot\boldsymbol{u}|^2 + h^2(\boldsymbol{u}) + k^2(\boldsymbol{u}) \tag{28}$$

for

$$\begin{aligned} h^2(\boldsymbol{u}) &= \begin{vmatrix} v_{xy} & u_{xy} \\ \overline{\Delta}_{xy}v & \overline{\Delta}_{xy}u \end{vmatrix} \\ &\quad + \begin{vmatrix} w_{xy} & v_{xy} \\ \overline{\Delta}_{yz}w & \overline{\Delta}_{yz}v \end{vmatrix} \\ &\quad + \begin{vmatrix} u_{xy} & w_{xy} \\ \overline{\Delta}_{zx} & \overline{\Delta}_{zx}w \end{vmatrix} \end{aligned} \tag{29}$$

$$k^2(\boldsymbol{u}) = div\boldsymbol{s},\ \boldsymbol{s} = \begin{pmatrix} \begin{vmatrix} v_y & w_y \\ v_z & w_z \end{vmatrix} \\ \begin{vmatrix} w_z & u_z \\ w_x & u_x \end{vmatrix} \\ \begin{vmatrix} u_x & v_x \\ u_y & v_y \end{vmatrix} \end{pmatrix} \tag{30}$$

where

$$\Delta_{\alpha\beta} = \frac{\partial^2}{\partial\alpha^2} + \frac{\partial^2}{\partial\beta^2},\ \overline{\Delta}_{\alpha\beta} = \frac{\partial^2}{\partial\alpha^2} - \frac{\partial^2}{\partial\beta^2} \tag{31}$$

for $\alpha, \beta \in \{xy, yz, zy\}$. These relations show that $tr\boldsymbol{H}\boldsymbol{H}^{\top}$, and $|\nabla div\boldsymbol{u}|^2$ and $|\nabla rot\boldsymbol{u}|^2$ are dependent terms. Therefore, considering the regularisation term $tr\boldsymbol{H}\boldsymbol{H}^{\top}$ is equivalent to solve vector spline minimisation for optical flow computation.

Setting

$$\boldsymbol{S}_k = D^k f D^k f^{\top} \tag{32}$$

we define the k-th order Nagel-Enkelmann regulariser.

Definition 1. *The k-th order Nagel-Enkelmann regulariser is*

$$J_{kNE} = trD^k\boldsymbol{u}\boldsymbol{N}_k D^k\boldsymbol{u}^{\top}, \tag{33}$$

where

$$\boldsymbol{N}_k = \frac{1}{tr\boldsymbol{S}_k + n\lambda^2}((tr\boldsymbol{S}_k)\boldsymbol{I} - \boldsymbol{S}_k + (n-1)\lambda^2\boldsymbol{I}). \tag{34}$$

For $k = 1$, eq. (33) becomes the Nagel-Enkelmann regulariser.

A generalisation of the Nagel-Enkelmann method for optical-flow computation is achieved by minimising the criterion

$$\begin{aligned} J_{\infty} &= \int_{\mathbf{R}^n} \{|\nabla f^{\top}\boldsymbol{u} + f_t|^2 \\ &\quad + \sum_{k=1} \beta_k tr D_k\boldsymbol{u}\boldsymbol{N}_k D^k\boldsymbol{u}^{\top}\Big\}\, d\boldsymbol{x} \end{aligned} \tag{35}$$

and the associated Euler-Lagrange equation is,

$$\begin{aligned} &(\nabla f^{\top}\boldsymbol{u} + f_t)\nabla f \\ &+ \sum_{k=1}(-1)^k\beta_k D^{k\top}\boldsymbol{N}_k D^k\boldsymbol{u} = 0 \end{aligned} \tag{36}$$

since

$$\frac{\delta}{\delta f}trD^k\boldsymbol{u}\boldsymbol{N}_k D^k\boldsymbol{u} = (-1)^k D^{k\top}\boldsymbol{N}_k D^k\boldsymbol{u} \tag{37}$$

for symmetry matrices $\boldsymbol{N}_k$ $k \geq 1$.

4 Classification of Points by Motion

Let $\boldsymbol{u}^*_{(\alpha\beta\gamma)}$ be the optical flow vector computed using α-th, β-th, and γ-th constraints. For each point $\boldsymbol{x}$, we can have many optical-flow vectors $\boldsymbol{u}^*_{(\boldsymbol{\alpha})}$, where $\boldsymbol{\alpha}$ is a string of positive integers, for example, 1, 2, 12, 123, and so on. The vector $\boldsymbol{u}^*_{(2)}$ is the deformation vector of the deformable boundary. Therefore, if $|\boldsymbol{u}^*_2|$ is sufficiently small at point $\boldsymbol{x}$, and $\boldsymbol{u}^*_{(1)} \gg \boldsymbol{u}^*_{(2)}$ the motion in the neighbourhood of this point $\boldsymbol{x}$ is homogeneous. This geometrical property of optical-flow computed by the variational method implies that the operation

$$\mathbf{D}_{(i)} = \{\boldsymbol{x} \,|\, |\boldsymbol{u}^*_{(i)}| \gg |\boldsymbol{u}^*_{(j)}|, i \neq j\} \tag{38}$$

derives segments in $\mathbf{R}^n$ using the orders of constraints for the computation of variational problems. Generally, it is possible to adopt many constraints for the classification of moving points in a space with optical-flow vectors. For example, two operations

$$\mathbf{D}_{\text{homogeneous}} = \{\boldsymbol{x} \,|\, |\boldsymbol{u}^*_{(1)}| \gg |\boldsymbol{u}^*_{(12)}|\}, \tag{39}$$

$$\mathbf{D}_{\text{deform}} = \{\boldsymbol{x} \,|\, |\boldsymbol{u}^*_{(12)}| \gg |\boldsymbol{u}^*_{(1)}|\} \tag{40}$$

classify a scene into a deforming part and a homogeneously moving part, since the regularisers $tr\nabla\boldsymbol{u}\nabla\boldsymbol{u}^\top$ and $trD^2\boldsymbol{u}D^2\boldsymbol{u}^\top$ minimise smoothness and elastic energy of the solution $\boldsymbol{u}$, respectively. Furthermore, the operation

$$\boldsymbol{u} = \begin{cases} \boldsymbol{u}^*_{(1)}, & \text{if } |\boldsymbol{u}^*_{12}| \ll 1 \text{ on } \boldsymbol{x}, \\ \boldsymbol{u}^*_{(12)}, & \text{otherwise,} \end{cases} \tag{41}$$

allows us to express multi-modal motion simultaneously, using variational computation methods. These properties imply that the orders of the constraints in variational problems act as the scale of scale space analysis.

5 Numerical Scheme and its Stability

Setting $\boldsymbol{D}^2$ and $\boldsymbol{D}^4$ to be numerical operations stand for ∇^2 and ∇^4, respectively, we have the next numerical PDE of the fourth order

$$\frac{\boldsymbol{u}^{n+1} - \boldsymbol{u}^n}{\Delta\tau} = \boldsymbol{D}^2\boldsymbol{u}^n - \frac{\beta}{\alpha}\boldsymbol{D}^4\boldsymbol{u}^n - \frac{1}{\alpha}(\nabla f^\top \boldsymbol{u}^{n+1} + f_t)\nabla f \tag{42}$$

From this numerical PDE we have the iterative form

$$\begin{aligned} \boldsymbol{u}^{n+1} &= \left(\boldsymbol{I} + \frac{\Delta\tau}{\alpha}\nabla f\nabla f^\top\right)^{-1} \\ &\quad \times \left(\boldsymbol{I} + \Delta\tau\boldsymbol{D}^2 - \Delta\tau\frac{\beta}{\alpha}\boldsymbol{D}^4\right)\boldsymbol{u}^n \\ &\quad - \frac{\Delta\tau}{\alpha} f_t \left(\boldsymbol{I} + \frac{\Delta\tau}{\alpha}\nabla f\nabla f^\top\right)^{-1}\nabla f. \end{aligned} \tag{43}$$

Let

$$\boldsymbol{A} = \left(\boldsymbol{I} + \frac{\Delta\tau}{\alpha}\nabla f\nabla f^\top\right), \tag{44}$$

$$\boldsymbol{B} = \left(\boldsymbol{I} + \Delta\tau\boldsymbol{D}^2 - \Delta\tau\frac{\beta}{\alpha}\boldsymbol{D}^4\right). \tag{45}$$

If

$$\rho\left(\boldsymbol{B}^{-1}\boldsymbol{A}\right) < 1, \tag{46}$$

then the iterative form eq. (43) is stable and converges to the solution of the original equation. From the relations

$$\rho\left(\boldsymbol{B}^{-1}\boldsymbol{A}\right) \leq \rho\left(\boldsymbol{B}^{-1}\right)\rho\left(\boldsymbol{A}\right) \tag{47}$$

and $\rho\left(\boldsymbol{B}^{-1}\right) = 1$, if $\rho\left(\boldsymbol{A}\right) < 1$, the relation of eq. (46) is satisfied.

Setting $\boldsymbol{U}$ and $\boldsymbol{\Lambda}$ to be an orthogonal matrix and diagonal matrix respectively, we have the relations

$$\boldsymbol{D}^2 = \boldsymbol{U}\boldsymbol{\Lambda}\boldsymbol{U}^\top, \quad \boldsymbol{D}^4 = \boldsymbol{U}\boldsymbol{\Lambda}^2\boldsymbol{U}^\top. \tag{48}$$

Substituting these relations to

$$\rho\left(\boldsymbol{I} + \Delta\tau\boldsymbol{D}^2 - \Delta\tau\frac{\beta}{\alpha}\boldsymbol{D}^4\right) < 1 \tag{49}$$

we have the relation

$$\rho\left(\boldsymbol{U}\left(\boldsymbol{I} + \Delta\tau\boldsymbol{\Lambda} - \Delta\tau\frac{\beta}{\alpha}\boldsymbol{\Lambda}^2\right)\boldsymbol{U}^\top\right) < 1 \tag{50}$$

Then, finally we have the convergence condition

$$\rho\left(\boldsymbol{I} + \Delta\tau\boldsymbol{\Lambda} - \Delta\tau\frac{\beta}{\alpha}\boldsymbol{\Lambda}^2\right) < 1. \tag{51}$$

Since the diagonal coefficients of $\boldsymbol{\Lambda}$ and $\boldsymbol{\Lambda}^2$ exist in the intervals $[-4n/h^2, 0]$ and $[0, 16n^2/h^4]$, where n is the dimensional the problem, we have the relation

$$\rho\left(\boldsymbol{I} + \Delta\tau\boldsymbol{\Lambda} - \Delta\tau\frac{\beta}{\alpha}\boldsymbol{\Lambda}^2\right) \leq \left|1 - 4n\frac{\Delta\tau}{h^2} - 16n^2\frac{\beta}{\alpha}\frac{\Delta\tau}{h^4}\right|. \tag{52}$$

From eq. (52), we have the next theorem.

Theorem 1. *If the inequality*

$$\left|1 - 4n\frac{\Delta\tau}{h^2} - 16n^2\frac{\beta}{\alpha}\frac{\Delta\tau}{h^4}\right| \leq 1 \tag{53}$$

is satisfied, the iterative form is stable and converges to the solution of the original PDE.

This theorem derives the next corollaries.

Corollary 1. *If $h = 1$, the convergence condition is*

$$0 \leq \Delta\tau \leq \frac{1}{2n + 8n^2\frac{\beta}{\alpha}}. \tag{54}$$

If $n = 2$, $\beta = \alpha$, and $h = 1$, the convergence condition is

Corollary 2. *If $n = 2$, $\beta = \alpha$, and $h = 1$, the convergence condition is*

$$\Delta\tau \leq \frac{1}{36} \tag{55}$$

Corollary 3. *If $n = 3$, $\beta = \alpha$, and $h = 1$, the convergence condition is*

$$\Delta\tau \leq \frac{1}{78} \tag{56}$$

It is possible to define Nagel-Enkelmann term for any dimensions as

$$\boldsymbol{N}_k = \frac{1}{tr\boldsymbol{S}_k + n\lambda^2}((tr\boldsymbol{S}_k)\boldsymbol{I} - \boldsymbol{S}_k + (n-1)\lambda^2\boldsymbol{I}), \tag{57}$$

where $\boldsymbol{S}_k = D^k f D^k f^\top$.

For $\boldsymbol{N}_k$, we have the relations

$$\boldsymbol{N}_D^k f = \frac{(n-1)\lambda^2}{|D^k f|^2 + n\lambda^2} D^k f, \tag{58}$$

$$\boldsymbol{N}_k D^k f^\perp = \frac{|D^k f|^2 + (n-1)\lambda^2}{|D^k f|^2 + n\lambda^2} D^k f^\perp, \tag{59}$$

Therefore, setting $n(k) = n^k$, it is possible to derive the eigenvalue decompositions of $\boldsymbol{N}$ as

$$\boldsymbol{N}_k = \boldsymbol{R}diag(d_1, d_2, \cdots, d_{n(k)})\boldsymbol{R}^\top \tag{60}$$

for $\boldsymbol{R} = (\boldsymbol{r}_1, \boldsymbol{r}_2 \cdots, \boldsymbol{r}_{n(k)})^\top$, where

$$\boldsymbol{r}_1 = \frac{D^k f}{|D^k f|}, \ \boldsymbol{r}_k^\top \boldsymbol{r}_1 = 0, \tag{61}$$

for $k \geq 2$ and

$$d_1 = \frac{(n-1)\lambda^2}{|D^k f|^2 + n\lambda^2},$$
$$d_2 = \cdots = n_n = \frac{|D^k f|^2 + (n-1)\lambda^2}{|D^k f|^2 + n\lambda^2}, \tag{62}$$

Therefore, we have the relation

$$0 \leq \rho(\boldsymbol{N}_k) \leq 1. \tag{63}$$

This relation means that a numerical scheme for the higher order Horn-Schunck constraints satisfies the convergence condition, the higher order Nagel-Enkelmann constraints satisfies the convergence condition.

6 Numerical Examples

Figure 1 shows the results of constraint-based classification of motion for Marble Block sequence. In (b), (c) and (d), the parameters are selected as $\alpha = 10^4, \beta = 0$, $\alpha = 10^4, \beta = 5 \times 10^3$, and $\alpha = 1, \beta = 10^4$, respectively. If $\beta = 0$, that is, without thr second order constraint, the algorithm extractes smooth motion all over the scean. However, if the ratio $\frac{\beta}{\alpha}$ is large, the algorithm extracts the motion on the segment-boundaries. This property is based on the analytical properties of the thin-plate spline constraint which allows us to detect the bendings of the object surfaces. Therefore, if β is small or zero the algorithm detects the motionof textured areas. And if β is large, the algorithm detects the motion of segment-boundaries.

Figure 2 shows optical flow on $\mathbf{R}^2$ computed using the Horn-Schunck regulariser with the first-order constraint and the Horn-Schunck regulariser with the first and second order regularisers. We detected the motion of clouds in a typhoon sequence. (a) shows the first frame in the sequence. Optical-flow fields in (b) and (c) are computed from the first and the second frames. (b) shows optical flow computed using the first-order constraint for $\alpha = 1000$. (c) shows optical flow computed using the first- and second- order constraints for $\alpha = \beta = 1000$. In the computed vector field in (b), the motion of cloud at the front and the boundary of the typhoon is detected. In these parts of a typhoon, clouds move as the boundary of deformable objects. Therefore, the second order constraints, which minimises elastic energy of the boundary in an images, allows us to detect the motion of clouds in front of typhoon in an image.

In Figure 3, (a) shows optical flow computed by the Horn-Schunck. We set $\alpha = 5 \times 10^5$ and $\frac{\Delta\tau}{\Delta x^2} = 0.166$. The factor $\frac{\Delta\tau}{\Delta x^2} = 0.166$ satisfies the convergence condition of the iterative form. (b) is the result of optical flow computed with the first and second Horn-Schunck regularisers, setting $\alpha = 10^6$ and $\beta = 5 \times 10^5 = \alpha/2$. The convergence condition is derived by the Lax equivalence law. The parameter α is select so that the absolute values of the first and second terms of the diffusion equation for optical-flow computation are numerically equivalent. From these results, we can see that the flow-vector field extracted by the Horn-Schunck regulariser are smooth in the neighbourhood of each point. Furthermore, the result in (b) extracted the deformable parts of the heart using the second order constraint. This result suggests the decomposition of the region on the surface of the heart to the deforming regions and homogeneous moving regions.

7 Conclusions

We have introduced variational constraints with higher order derivatives for vector-valued functions. Using the higher order constraints, we have introduces the constraint-based motion classification for optical-flow vectors.

The constraints based on the second derivatives for the terrain function $z = f(x, y)$ in three-dimensional Euclidean space is used in the elastic theory [7]. The

constraints with the higher order derivatives in variational problems leads to the conclusion that the second order vector-spline constraint for optical-flow computation is mathematically replaceable to a quadric form of the second order derivatives of the solution. This replacing of constraint derives a fourth order diffusion-reaction equation for optical-flow computation. This fourth order diffusion-reaction equation is numerically solved using the same scheme with computation of the usual diffusion equation. Furthermore, we have introduced the Nagel-Enklmann type constraints for the higher order derivatives using the higher order derivatives of the image.

The higher order data consistencies are

$$\frac{d}{dt}D^k f = 0,\ k \geq 1. \tag{64}$$

Equation (64) is rewritten as

$$D^k \nabla^\top f + D^k f_t = 0 \tag{65}$$

in the matrix form. For instance, if we set $k = 0$ and $k = 1$, we have the illumination consistency

$$\nabla f^\top \boldsymbol{u} + f_t = 0 \tag{66}$$

and the gradient consistency

$$\nabla\nabla^\top f\boldsymbol{u} + \nabla f_t = 0. \tag{67}$$

Therefore, setting the higher order data consistencies and the higher order smoothness constraints as

$$E_D = \sum_{i=0}^{\infty} \lambda_i (D^i \nabla^\top f\boldsymbol{u} + D^i f_t)^2 \tag{68}$$

and

$$E_S = \sum_{j=1}^{\infty} \alpha_j D^j \boldsymbol{u}^\top \boldsymbol{N}_j D^j \boldsymbol{u} \tag{69}$$

for appropriate non-negative constants $\Lambda = \{\lambda_i\}_{i=0}^{\infty}$ and $A = \{\alpha_i\}_{j=1}^{\infty}$, we define a general optimisation problem for optical-flow computation as

$$J(\boldsymbol{u}) = \int_{\mathbf{R}^n} (E_D + E_S)\, d\boldsymbol{x}. \tag{70}$$

The solution of the problem is the solution of the PDE

$$\sum_{j=1}^{\infty} (-1)^{j+1} \alpha_j D^{j\top} \boldsymbol{N}_j D^j \boldsymbol{u} + \sum_{i=0}^{\infty} \lambda_i D^i \nabla^\top f (D^i \nabla^\top f\boldsymbol{u} + D^i f_t) = 0, \tag{71}$$

where $[D^p D^{q\top}]f$ is a $n^p \times n^q$ matrisation of the Hessian matrix $\boldsymbol{H}_{p+q}$ of f.

For the optimisation problem of eq. (70), we define the problem.

$$\boldsymbol{u}_{(\alpha,\lambda)} = \text{argument min}\, J(\boldsymbol{u}; \alpha \subseteq A, \lambda \subseteq \Lambda). \tag{72}$$

We call the solution of this problem the (α, λ) optical flow. The optical-flow vectors which we have dealt with in this paper are $(0, 1)$ and $(0, 12)$ optical flow vectors. For the detection of the motion boundaries, the gradient consistency drives acceptable results. Therefore, we will deal with $(01, 1)$ and $(01, 12)$ optical flow vectors.

The optical-flow field is a sequence of vector-valued function. For segmentation, smoothing, in-printing, and denoising of the vector-valued functions, it is possible to use variational method. A variational criterion for the vector-valued function is expressed as

$$J_{1\text{noise}}(\boldsymbol{u}) = \int_{\mathbf{R}^n} \left\{ |\boldsymbol{f} - \boldsymbol{u}|^2 + \alpha tr \nabla\boldsymbol{u}\nabla\boldsymbol{u}^\top \right\} d\boldsymbol{x}. \tag{73}$$

A generalisation is

$$J_{\infty\text{noise}}(\boldsymbol{u}) = \int_{\mathbf{R}^n} \left\{ |\boldsymbol{f} - \boldsymbol{u}|^2 + \sum_{k=1}^{\infty} \frac{\tau^k}{k!} tr D^k \boldsymbol{u} D^k \boldsymbol{u}^\top \right\} d\boldsymbol{x}. \tag{74}$$

The Euler-Lagrange equation of this minimisation problem is

$$\boldsymbol{f} - \boldsymbol{u} + \sum_{k=1}^{\infty} \frac{(-1)^k \tau^k}{k!} \Delta^k \boldsymbol{u} \tag{75}$$

we have the formal equation

$$\boldsymbol{f} = \exp(-\tau\Delta)\boldsymbol{u}. \tag{76}$$

Therefore, we have the solution

$$\boldsymbol{u} = \exp(\tau\Delta)\boldsymbol{f}. \tag{77}$$

This relation implies that $\boldsymbol{u}$ is the solution of

$$\frac{\partial \boldsymbol{u}}{\partial \tau} = \Delta\boldsymbol{u},\ \boldsymbol{u}(\cdot, 0) = \boldsymbol{f}. \tag{78}$$

References

[1] Weickert, J., Bruhn, A., Papenberg, N., Brox, T., Variational optic flow computation: From continuous models to algorithms, Proceedings of International Workshop on Computer Vision and Image Analysis, IWCVIA'03, 2003.

[2] Aubert, G., Kornprobst, P., *Mathematical Problems in Image Processing:Partial Differential Equations and the Calculus of Variations,* Springer, 2002.

[3] Barron, J. L., Fleet, D. J., Beauchemin, S. S., Performance of optical flow techniques, International Journal of Computer Vision, **12**, 43-77, 1994.
[4] Horn, B. K. P., Schunck, B. G., Determining optical flow, Artificial Intelligence, **17**, 185-204, 1981.
[5] Nagel, H.-H., On the estimation of optical flow: Relations between different approaches and some new results. Artificial Intelligence, **33**, 299-324, 1987.
[6] Weickert, J., Schnörr, Ch., Variational optic flow computation with a spatio-temporal smoothness constraint, Journal of Mathematical Imaging and Vision **14**, 245-255, 2001.
[7] Timoshenko, S. P., *History of Strength of Materials*, Dover, 1983.
[8] Steidl, G., Didas, S., Neumann J., Splines in higher order TV Regularization, IJCV, **70**, 241-255, 2006.
[9] Grenander, U., Miller, M., Computational anatomy: An emerging discipline, Quarterly of applied mathematics, **4**, 617-694, 1998.
[10] Sorzano, C. Ó. S.,, Thévenaz, P., Unser, M., Elastic registration of biological images using vector-spline regularization, IEEE Tr. Biomedical Engineering, **52**, 652-663, 2005.
[11] Wahba, G., Wendelberger, J., Some new mathematical methods for variational objective analysis using cross-validation, Monthly Weather Review, **108**, 36-57, 1980.
[12] Amodei, L., Benbourhim, M. N., A vector spline approximation, Journal of Approximation Theory, **67**, 51-79, 1991.
[13] Benbourhim, M. N., Bouhamidi, A., Approximation of vectors fields by thin plate splines with tension, Journal of Approximation Theory, **136**, 198-229, 2005.
[14] Suter, D., Motion estimation and vector spline, Proceedings of CVPR'94, 939-942, 1994.
[15] Selig, J. M., *Geometrical Method in Robotics*, Springer, 1996.

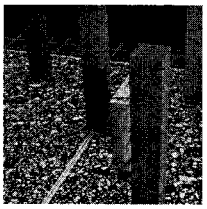

(a)

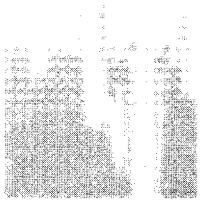

(b)

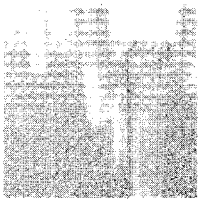

(c)

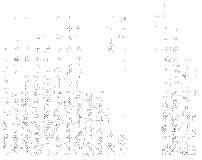

(d)

Figure 1: Results of Flow Vector Classification. (a) is an original image. (b) $\alpha = 10^4, \beta = 0$, (c) $\alpha = 10^4, \beta = 5 \times 10^3$, (d) $\alpha = 1, \beta = 10^4$. If $\beta = 0$, that is, without thr second order constraint, the algorithm extractes smooth motion all over the scean. However, if the ratio $\frac{\beta}{\alpha}$ is large, the algorithm extracts the motion on the segment-boundaries.

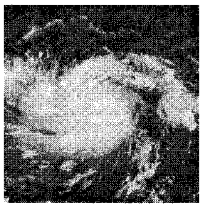

(a)

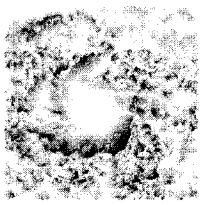

(b)

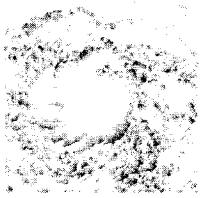

(c)

Figure 2: Optical Flow of Clouds in a Typhoon Sequence. (a) shows the first frame in the sequence. Optical-flow fields in (b) and (c) are computed from the first and the second frames. (b) shows optical flow computed using the first-order constraint for $\alpha = 1000$. (c) shows optical flow computed using the first- and second- order constraints for $\alpha = \beta = 1000$.

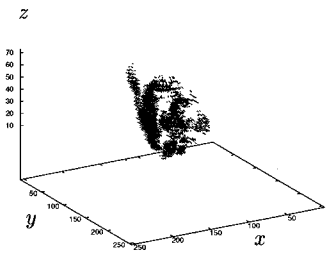

(a)

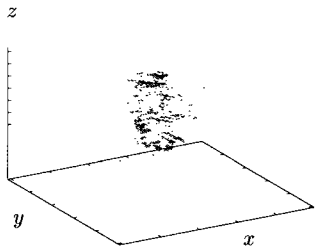

(b)

Figure 3: Optical Flow in $\mathbf{R}^3$. From top to bottom, optical flow computed by the Horn-Schunck constraint (a). We set $\alpha = 5 \times 10^5$, $\frac{\Delta\tau}{\Delta x^2} = 0.166$, and $\lambda = 1$. (b) is the result of optical flow computed with the first and second Horn-Schunck regularisers, setting $\alpha = 10^6$ and $\beta = 5 \times 10^5 = \alpha/2$.